Reaction cross sections for $^{14}N + ^{10}B$

P. A. DeYoung,* J. J. Kolata, L. J. Satkowiak, and M. A. Xapsos
Physics Department, University of Notre Dame, Notre Dame, Indiana 46556
(Received 4 February 1983)

Excitation functions for the yields of nineteen residual nuclei from the $^{14}N + ^{10}B$ reaction have been measured over the range $E_{c.m.} = 8.00$–25.75 MeV in steps of 250 keV with γ-ray techniques. The magnitude and energy dependence of the excitation functions for the partial yields are very different from those of the $^{12}C + ^{12}C$ system. The total fusion cross section appears to saturate at an energy and a magnitude which are lower than expected from previous systematics. Small, regular fluctuations can be seen in the fusion cross section, one of which is very narrow. However, the structure observed by L'Ecuyer *et al.* was not seen in this work.

[NUCLEAR REACTIONS $^{10}B(^{14}N,x)$; $E_{c.m.} = 8.00$–25.75 MeV; measured excitation functions for the production of $A = 10$–23 reaction products; observed small fluctuations at $E_{c.m.} = (10.8)$, 11.9, 13.9, 15.7, 16.3, and 18.7 MeV; deduced critical angular momentum for fusion.]

I. INTRODUCTION

The fusion cross section for reactions producing compound systems in the $A = 24$–32 region has been found to account for most of the expected reaction cross section in the energy region just above the Coulomb barrier. However, at some point, the behavior of the fusion cross section with energy is observed to diverge from that of the reaction cross section. The location of this saturation point, and the behavior of the excitation function near it, have been the subject of much discussion and work. It has been found that many systems in this mass region show resonantlike structures in the measured excitation functions in the vicinity of the saturation point, despite the very high level density in the corresponding excited compound system which should preclude resonant behavior.

In an attempt to understand these phenomena, we have investigated several different reactions which lead to the same compound nucleus. In particular, the $^{16}O + ^{16}O$ and $^{12}C + ^{20}Ne$ reactions[1] and the $^{12}C + ^{16}O$ and $^{14}N + ^{14}N$ reactions[2] have been compared and contrasted in two recent experiments. The former pair, which form the ^{32}S compound system, are well matched in terms of Q value and angular momentum. The excitation functions for the total fusion cross section were found to exhibit similar behavior when compared at equal compound nucleus excitation energies, and both systems also displayed pronounced resonantlike structure. The latter pair, which form the ^{28}Si compound nucleus, are poorly matched systems. In this case the excitation functions for the total fusion cross section were found to exhibit average behavior which was quite different. The $^{14}N + ^{14}N$ reaction did show evidence for fluctuations, but at a much lower level than observed for the $^{12}C + ^{16}O$ system.

The $^{12}C + ^{12}C$ and $^{14}N + ^{10}B$ reactions (the ^{24}Mg compound system) provide an opportunity to compare the behavior of the fusion cross sections for yet another pair of entrance channels which are also very mismatched in terms of Q value and angular momentum. The $^{14}N + ^{10}B$ reaction brings 14.9 MeV more energy into the compound nucleus for a given center-of-mass energy but, since the sizes of the nuclei involved are similar, the angular momentum at a given center-of-mass energy is approximately the same for both entrance channels. As a result, very different regions of the compound nucleus with very different level densities are populated in the two reactions. In addition, $^{14}N + ^{10}B$ is an asymmetric system, while the corresponding $^{12}C + ^{12}C$ entrance channel consists of identical spin zero bosons. These systems also differ in the intrinsic spin and nuclear structure of the participating nuclei, and in the maximum available channel spin. In particular, the $^{14}N + ^{10}B$ system has up to $4\hbar$ units of channel spin available for coupling with the orbital angular momentum, while for the $^{12}C + ^{12}C$ system the final spin of the compound system is determined by the orbital momentum alone.

In this work, excitation functions have been measured for a large number of residual nuclei which result from the $^{14}N + ^{10}B$ reaction. The energy step size was small in order to detect resonantlike fluctuations, but a large energy range was covered to determine the long range behavior of the fusion cross section. The behavior of the excitation functions and the trajectory of the critical angular momentum for the $^{14}N + ^{10}B$ system were found to be very different from those for the $^{12}C + ^{12}C$ system. Small fluctuations were seen in the total fusion yield for $^{14}N + ^{10}B$. One of these is narrow and bears a remarkable resemblance to a similar structure seen in the $^{12}C + ^{20}Ne$ reaction.

II. EXPERIMENTAL METHOD AND RESULTS

The experiment was performed with a ^{14}N beam from the Notre Dame three-stage tandem Van de Graaff accelerator. The range of incident energies was $E_{c.m.} = 8.00$–25.75 MeV, with a step size of 250 keV. The target typically consisted of 50 $\mu g/cm^2$ of ^{10}B evaporated onto a thick Au backing and then covered with 10 $\mu g/cm^2$ of Au to reduce subsequent oxidation of the boron. In spite of these precautions, it was found that there

was a measurable amount of oxygen contamination in the target. To correct for this contamination, the $^{14}N + ^{16}O$ reaction was separately measured with a Ta_2O_5 target over the same energy range, and the affected yields from the $^{14}N + ^{10}B$ reaction were deduced accordingly. The relative normalization between these two experiments was determined from the yield of the 390 keV line of ^{25}Mg, which can only result from the $^{14}N + ^{16}O$ reaction. Carbon buildup on the ^{10}B target was minimized by surrounding the target with a liquid nitrogen cold trap and by maintaining a vacuum of $< 10^{-6}$ Torr in the target chamber. The target was periodically inspected and was always found to be free of any darkening due to carbon buildup. Also, the excellent agreement between the repeat points taken at the end of the experiment and the original points measured over the course of the experiment (Figs. 1–6) indicate little, if any, change in the condition of the target during the experiment.

Gamma rays were detected by two Ge(Li) detectors (90 cm^3 and 104 cm^3) placed 7 cm from the target and at 55° and 125° with respect to the beam axis. The gains of the respective amplifiers were adjusted to optimize one detector for the lower energy γ rays (80–2500 keV), and the other for higher energy γ rays (200–6200 keV). Thus, almost all of the γ rays of interest were detected by both detectors, without sacrificing either the higher- or lower-energy transitions.

The primary relative normalization of the data, which was derived from the 279 and 547 keV transitions in ^{197}Au under the assumption that the Coulomb excitation cross section is locally smooth, agreed with that obtained from charge collection to within 2% (rms deviation). The long term behavior of the excitation functions was determined from charge collection, but was found to be in excellent agreement with the predictions of a thick target Winther-de Boer multiple Coulomb excitation program.[3] The absolute normalization of the yields from the $^{14}N + ^{10}B$ reaction was determined by a multistep process involving the $^{12}C + ^{16}O$, $^{10}B + ^{16}O$, and $^{16}O + ^{10}B$ reactions. The $^{12}C + ^{16}O$ reaction, when combined with known $^{12}C + ^{16}O$ cross sections,[4] gives a measure of the thickness of the tantalum oxide target. This information, along with the results from the $^{10}B + ^{16}O$ experiment, yields a measure of the $^{10}B + ^{16}O$ cross section, which can be combined with data from the $^{16}O + ^{10}B$ reaction to give a measure of the thickness of the ^{10}B target. Finally, the $^{14}N + ^{10}B$ measurements can be expressed in terms of absolute cross sections using this deduced target thickness. The beam energies for the various measurements were 40.0 MeV for $^{12}C + ^{16}O$, 29.656 MeV for $^{10}B + ^{16}O$, and 47.45 MeV for $^{16}O + ^{10}B$. In each case, the primary normalization of the beam intensity was derived from Coulomb excitation of the Au target backing as discussed in detail in Ref. 2. The estimated uncertainty in the absolute normalization for the $^{14}N + ^{10}B$ reaction cross sections is approximately 12% (Table I).

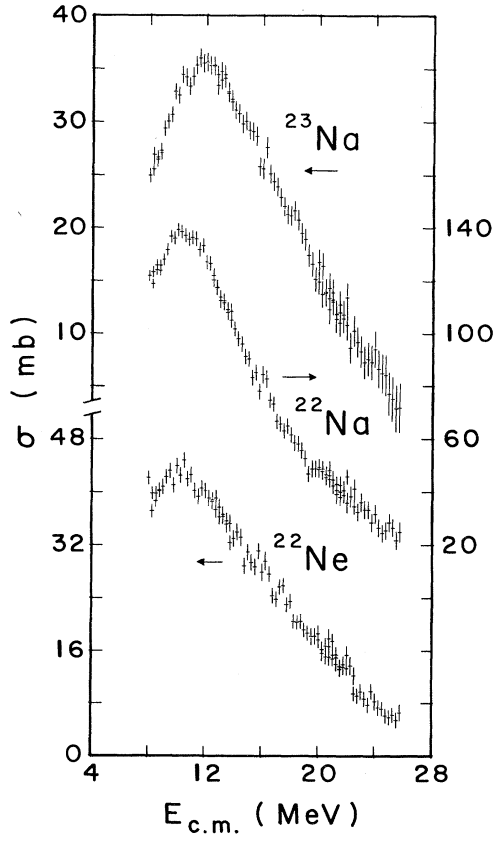

FIG. 1. The excitation functions for the production of $^{23,22}Na$ and ^{22}Ne.

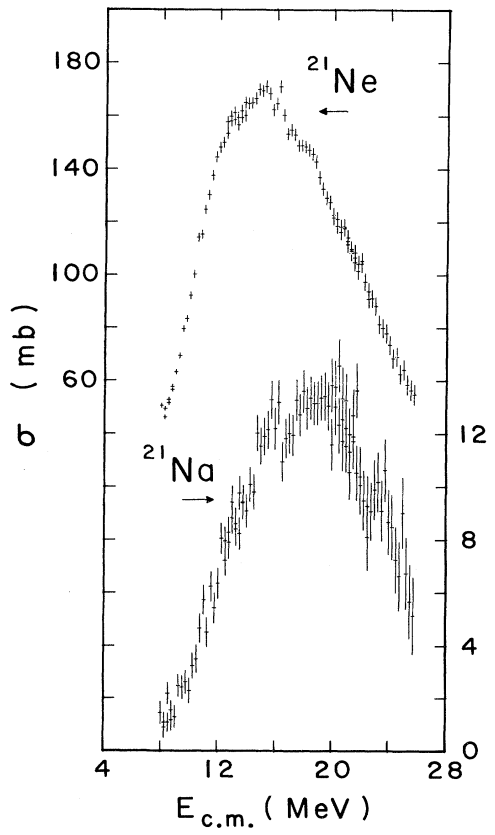

FIG. 2. The excitation functions for the production of ^{21}Ne and ^{21}Na.

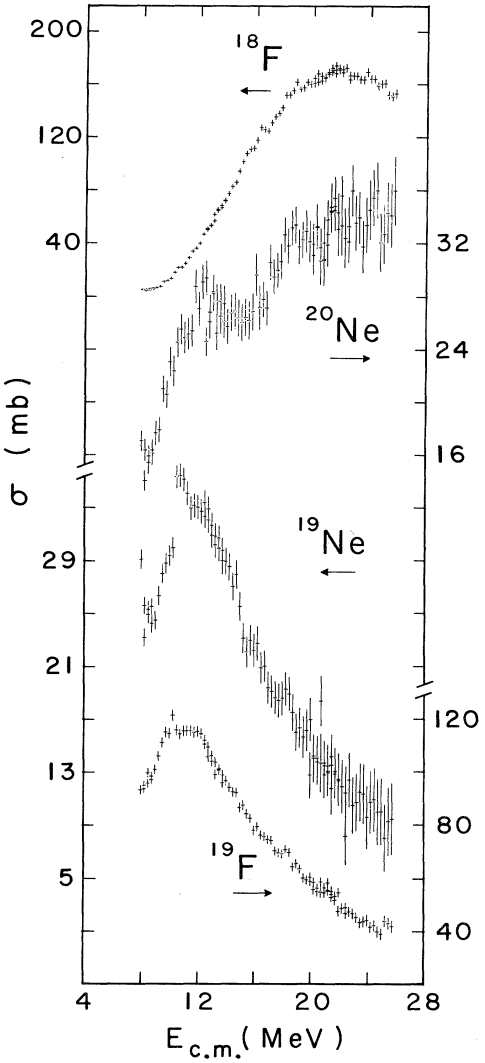

FIG. 3. The excitation functions for the production of ^{19,18}F and ^{20,19}Ne.

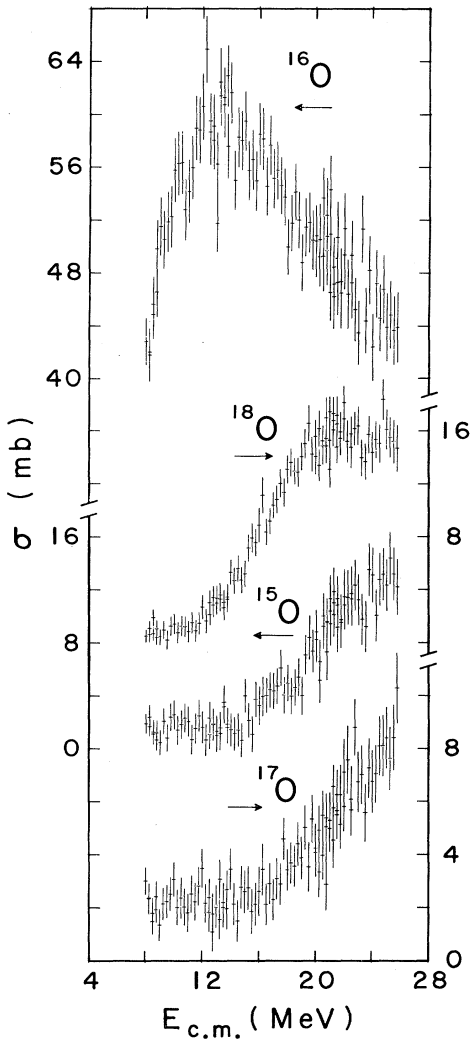

FIG. 4. The excitation functions for the production of ^{18,17,16,15}O.

The ground state transitions which were summed to determine the yields of the residual nuclei are shown in Table II. In an attempt to separate the contribution of the (nonground state) 1636 keV transition in ^{23}Na from that of the 1634 keV transition in ^{20}Ne, only that portion of the lineshape which was not Doppler broadened or Doppler shifted was integrated to form the ^{20}Ne excitation function. This separation is based on the lifetimes[5] of the two states involved (40 fs for the ^{23}Na line and 1.2 ps for that of ^{20}Ne) and the observation that other transitions involving similar lifetimes exhibited small stopped or shifted components, respectively.

Excitation functions for the production of ^{23}Mg, ^{23,22,21}Na, ^{22,21,20,19}Ne, ^{20,19,18}F, ^{18,17,16,15}O, ^{15,14}N, ^{12}C, and ^{10}B were measured. The strongest of these are shown in Figs. 1–5. (Those excitation functions not shown each have less than 10 mb of peak cross section throughout the energy range studied.) The excitation function for the total fusion yield (Fig. 6) was formed by summing the channels listed above, and including an estimate of the yield from the 2^+, 6919 keV state in ^{16}O based on the results of Ref. 6. This summing of all observed exit channels may mean that a small amount of direct reaction strength has been included under the label of fusion evaporation. However, at the highest energies of this work, the ^{10}B and ^{14}N yields, which should contain most of the direct strength as well as some fusion-evaporation components, amount to less than 30 mb out of a summed cross section of 700 mb. The error bars shown in Figs. 1–6 are the uncertainties in the peak areas added in quadrature to the rms deviation in the relative normalization, and include an estimated error in the contaminant subtraction process.

III. DISCUSSION

A. Comparison with other experiments

The results of the one previous measurement of the ^{14}N + ^{10}B system in this energy region are compared with this work in Table III. Parks *et al.*[7] using heavy-particle

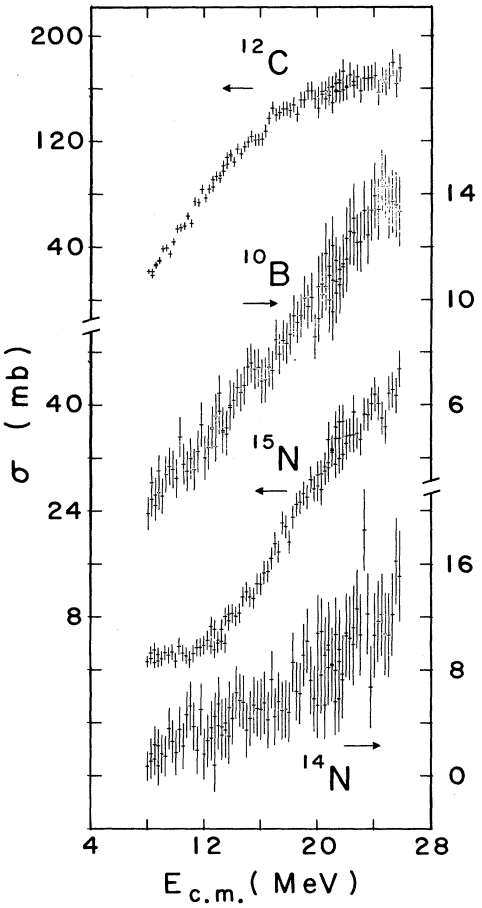

FIG. 5. The excitation functions for the production of ^{12}C, ^{10}B, and $^{15,14}N$.

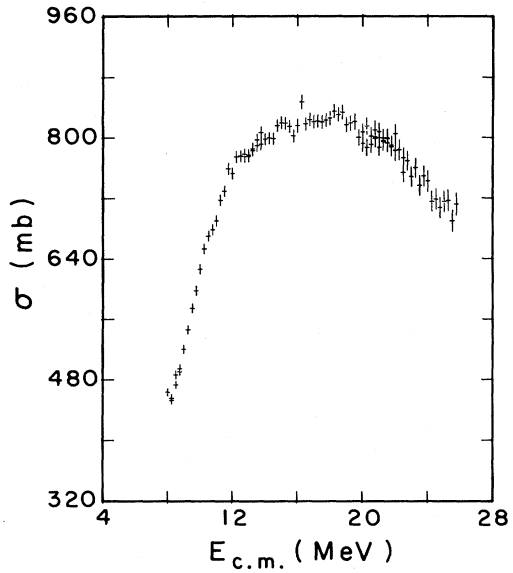

FIG. 6. The excitation function for the total fusion cross section.

detection techniques, measured the cross section for seven residual elements (Mg, Na, Ne, F, O, C, and B) at four energies, two of which overlap the energy range of this work. The agreement between the two works is good for most of the elemental yields. The cross sections given in Ref. 7 are generally smaller than those measured in the present experiment by 10%, which is well within the mutual systematic errors of the two experiments. On the other hand, we note that the major contribution to the uncertainty in the absolute yield in the present experiment is the magnitude of the $^{12}C + ^{16}O$ reference cross section. Relative to this standard, the cross sections presented here and in previous experiments (see Ref. 1, e.g.), are considerably more precise.

The most significant discrepancy between the present experiment and Ref. 7 occurs in the measured oxygen yield. At the higher energy, a difference of approximately 100 mb is observed, with the measurements of Parks *et al.* being the larger. In view of the rather good agreement for the other elemental yields, this observation is not easy to understand. The disagreement between the two measurements at $E_{c.m.}=21.1$ MeV, if it results from the fusion-evaporation process, must be due to differences in the yields of oxygen isotopes other than ^{16}O, since the ^{16}O residual nuclei result from two-particle evaporation (2α) and therefore should decrease at the higher energies as observed (Fig. 4). Three other oxygen isotopes (^{15}O, ^{17}O, and ^{18}O) were identified in our data. The yields of these nuclides do increase with increasing energy as expected (Fig. 4), but their summed cross section is quite small. It is possible that the observed difference is due to the inability of the γ-ray technique to measure direct population of the ground state. However, based on previous experience, and the relatively good agreement for other nuclides at both

TABLE I. Contributions to the uncertainty in the absolute normalization.

Source	Error (%)
Statistical error in the integration of the reference γ-ray line for $^{12}C + ^{16}O$	0.6
Statistical error in the integration of the γ-ray line for $^{10}B + ^{16}O$	0.9
Statistical error in the integration of the γ-ray line for $^{16}O + ^{10}B$	0.9
Statistical error in the integration of the γ-ray line for $^{14}N + ^{10}B$	0.7
Uncertainty in the Ge(Li) efficiency function	1.4
Uncertainty in the beam intensities	1.7
Statistical uncertainty in the reference cross section	2.7
Estimated uncertainty in the magnitude of the total yield due to contaminant subtraction	3.0
Total statistical uncertainty	4.8
Systematic uncertainty in the reference cross section	7.0

TABLE II. Ground-state γ-ray transitions observed from the $^{14}N + {}^{10}B$ reaction.

Nuclide	Evaporated particles	E_γ (keV)
^{23}Mg	n	451
^{23}Na	p	440
^{22}Na	pn	583, 891, 1526, 2571
^{21}Na	p2n	332
^{22}Ne	2p	1275
^{21}Ne	2pn	351
^{20}Ne	α[a,b]	1634
^{19}Ne	αn	238, 275
^{20}F	3pn	656
^{19}F	αp	110, 197
^{18}F	αpn[b]	937, 1081
^{18}O	$\alpha 2p$	1982
^{17}O	$\alpha 2pn$	821
^{16}O	2α[b]	6130
^{15}O	$2\alpha n$[b]	5241
^{15}N	$2\alpha p$[b]	5270
^{14}N	$2\alpha pn$[b]	5105
^{12}C	3α[b]	4440
^{10}B	$3\alpha pn$[b]	717

[a]The shape of the excitation functions suggests the possibility that ^{20}Ne may be formed by α evaporation at low energies, and by 2p2n evaporation at higher energies.
[b]This residue may also result from direct reaction processes.

TABLE III. Comparison of the measured yields of a given element from the $^{14}N + {}^{10}B$ reaction as given in Ref. 7 and the present experiment.

Exit channel	$E_{c.m.}$ (MeV)	σ (mb)[a] Ref. 7	σ (mb)[b] Present work
B	11.2	3.5	3.6±0.8
	21.2	14.0	11. ±1.
C	11.2	56.	74. ±3.
	21.2	116.	159. ±8.
N	11.2	14.[c]	6.2±2.2[d]
	21.2	81.	42. ±3.[d]
O	11.2	118.	116. ±4.
	21.2	227.	130. ±4.
F	11.2	93.	148. ±2.
	21.2	216.	233. ±3.
Ne	11.2	160.	190. ±2.
	21.2	174.	157. ±4.
Na	11.2	125.	176. ±3.
	21.2	50.	64. ±4.
Mg	11.2	9.3	4.8±0.5
	21.2	19.	10. ±1.

[a]No error was given for the elemental yields in Ref. 7. The uncertainty in the total fusion cross section is approximately 4—5 % at both of the energies listed above.
[b]The uncertainties given are the statistical errors only. The systematic uncertainty in the absolute normalization is 12%.
[c]Computed yield from the results of a Hauser-Feshbach Monte Carlo calculation.
[d]Total yield, with no separation as to fusion-evaporation or direct reaction. The yield due to inelastic scattering is estimated to be about 15% of the value given.

energies and for ^{16}O at 11.2 MeV, the magnitude of the difference seems much too large to be accounted for in this way. We note that the Ne yield at $E_{c.m.} = 21.2$ MeV, as given in Ref. 7, also seems to be larger than expected in view of the comparison of the two works at lower energy. The excitation function for production of Ne measured in this work is narrower than, and peaks at a lower energy than, that given by Parks *et al.*[7] A possible explanation for both of these discrepancies might be oxygen contamination of the ^{10}B target used in Ref. 7. As discussed above, it was found that the ^{10}B target used in the present experiment had a sizable oxygen contamination despite a protective Au layer and the fact that it was stored under vacuum. The effect of such contamination would become much more serious as the energy increases, since fusion evaporation from the $^{14}N + {}^{16}O$ system at high center-of-mass energies forms some of the same residual nuclei associated with the $^{14}N + {}^{10}B$ reaction, and in addition direct-reaction products from the $^{14}N + {}^{16}O$ system may also be confused with fusion yields from $^{14}N + {}^{10}B$. One last possibility is that the excess O and Ne yields in the experiment of Parks *et al.* result from incomplete-fusion processes which are selectively producing the ground states of the appropriate isotopes. If this is the case, then further study of the $^{14}N + {}^{10}B$ system, including a measure of the velocity profile of the reaction products, would be of some interest.

Finally, it should be noted that the N yield of Parks *et al.* is the result of a Hauser-Feshbach Monte Carlo calculation, while that given in this work is the result of direct measurement. The calculated N yield was included in the total fusion cross section reported by Parks *et al.* On the other hand, part of the N yield measured in this experiment undoubtedly results from direct reactions, making a comparison of the total fusion cross sections reported in the two works difficult to interpret.

The $^{14}N + {}^{10}B$ system has been studied at lower energies by Wu *et al.*[8] with γ-ray techniques, but the energy regions measured in Ref. 8 and this work do not overlap. Table IV gives the results of Wu *et al.* at their highest energy, and an extrapolation of the low-energy behavior of this work to a comparable energy. Although our yield functions have only been extrapolated by 0.5 MeV in c.m. energy, a considerable uncertainty must have been introduced into the comparison by the fact that most of the excitation functions are decreasing very rapidly with decreasing energy due to the influence of the Coulomb barrier. The cross section values listed in Ref. 8 were obtained by correcting certain measured yields according to branching ratios and summing factors deduced from a statistical-model calculation. The total fusion cross section has an additional (calculated) correction factor to account for unobserved three-particle evaporations based on the strengths of the two-particle evaporation yields. Despite the heavy reliance on such calculations in Ref. 8, the two experiments are generally seen to be in very good agreement. On the other hand, it is difficult to make a precise comparison considering the inherent problems with extrapolation procedures as discussed above.

B. Comparison with the $^{12}C + {}^{12}C$ system

Partially-smoothed excitation functions for many of the measured exit channels from the $^{14}N + {}^{10}B$ system are compared in Fig. 7 with the results of Kolata *et al.*[6]

TABLE IV. Comparison of the "measured" yields from the $^{14}N + ^{10}B$ reaction at $E_{c.m.}=7.5$ MeV. The data from the present experiment have been extrapolated from $E_{c.m.}=8.0$ MeV, which may introduce a considerable uncertainty due to the proximity of the Coulomb barrier as discussed in the text. This uncertainty is not reflected in the quoted errors, which are purely statistical.

Nuclide	σ (mb)[a] Ref. 8	σ (mb)[b] Present work
^{23}Mg	3.1± 0.5	3.0±0.4
^{23}Na	12.1± 0.5	22. ±1.
^{22}Na	102.0± 3.0	109. ±1.
^{22}Ne	31.4± 1.0	34. ±1.
^{21}Ne	36.2± 7.0	20. ±1.
^{20}Ne	7.0± 0.7	10. ±1.
^{19}Ne	16.2± 1.5	19. ±1.
^{19}F	79.3± 2.4	78. ±2.
^{16}O	91.0± 5.5	72.[c](39.[d]±2.)
Total fusion	472.±14.[e]	380.±5.[f]

[a]Adopted value including summing and branching ratio corrections. The errors quoted are statistical uncertainties. The overall systematic uncertainty in the absolute yield is ±15%.
[b]These values are an extrapolation of the low-energy data from this experiment to 7.5 MeV. The quoted uncertainty is the statistical error at the lowest energy measured in this work. The overall systematic uncertainty in the absolute normalization is estimated to be 12%.
[c]This value includes an estimate of the strength of the 2^+, 6919-keV yield.
[d]Measured yield of the 6130-keV γ ray.
[e]Includes a statistical-model estimate of several unmeasured three-particle emission cross sections. The estimated uncertainty in the absolute yield is ±20%.
[f]Includes all measured yields.

($E_{c.m.} > 17$ MeV) and Satkowiak *et al.*[9] ($E_{c.m.} < 17$ MeV) for the $^{12}C + ^{12}C$ system, as a function of the center-of-mass energy. In the case of the ^{32}S compound system previously studied, the corresponding excitation functions were found to compare favorably when plotted versus compound-nuclear excitation energy. The comparison for the ^{28}Si compound system was made at equivalent center-of-mass energies since the measured excitation functions for these poorly matched entrance channels showed some agreement when compared this way. For the present system, none of the excitation functions exhibit much similarity when compared either at equal center-of-mass energy or at equal compound-nuclear excitation energy, probably due to the very large Q-value difference between the two entrance channels, which is even larger here (10.6 MeV for the ^{28}Si compound system vs 15.0 MeV for ^{24}Mg) than in previous work.[2] This behavior can be qualitatively understood, just as for the ^{28}Si system, in terms of the vastly different excitation energy and angular momentum regions of the compound nucleus which are being populated by the two entrance channels. At a given center-of-mass energy, the angular momentum brought into the compound nucleus by each of the two entrance channels is very nearly equal, while the $^{14}N + ^{10}B$ channel carries in an extra 15 MeV of excitation energy. The increased internal energy which must be dissipated before the compound system reaches the point where γ-decay can compete with particle decay results in a tendency toward much longer evaporation sequences in the $^{14}N + ^{10}B$ system than for $^{12}C + ^{12}C$. Finally, we note that an examination of the total fusion excitation function (as well as the excitation functions of many of the residual nuclei) reveals fluctuations which will be discussed in the context of the critical angular momentum.

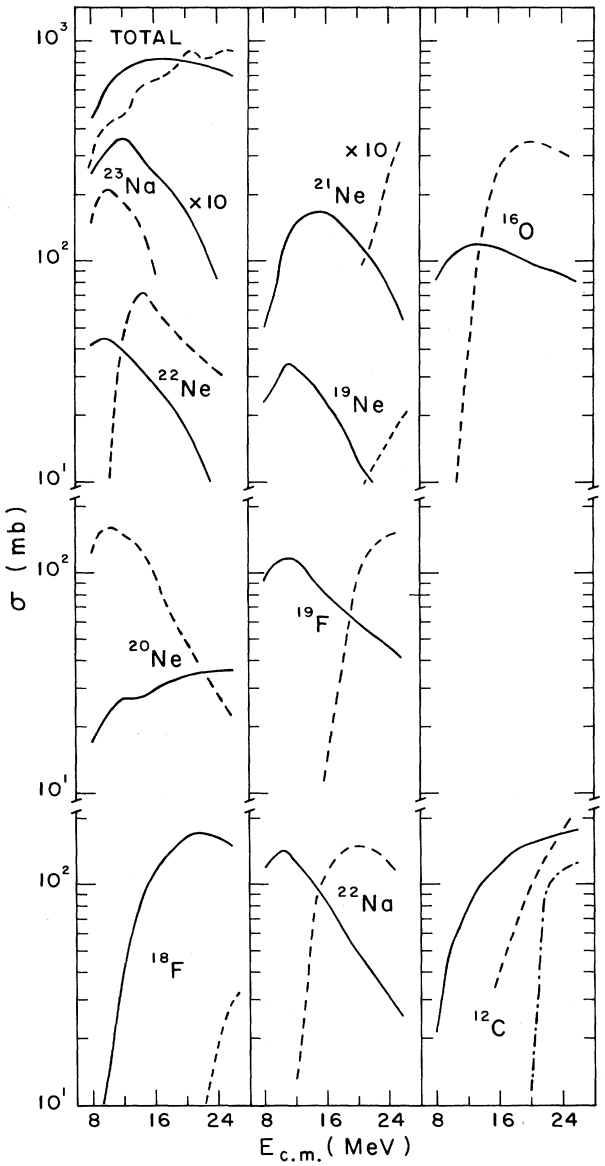

FIG. 7. Partially smoothed excitation functions for the $^{14}N + ^{10}B$ system (solid curve) and from the $^{12}C + ^{12}C$ system (Refs. 6 and 9, dashed curve), compared as a function of center-of-mass energy.

C. Trajectory of the critical angular momentum

The critical angular momentum (l_c) for a system of nonidentical particles is deduced from the total fusion cross section (σ_f) using the sharp-cutoff-model expression

$$\sigma_f = \pi \lambda\!\!\!^{-2} (l_c + 1)^2 , \quad (1)$$

where $\lambda\!\!\!^{-}$ is the reduced wavelength. The experimental values of l_c for the $^{14}N + {}^{10}B$ system deduced from the cross sections of Fig. 6 are shown in Fig. 8, along with the trajectory determined from the theoretical reaction cross section calculated with an optical-model potential.[10] In addition, the results from Ref. 11 for the $^{12}C + {}^{12}C$ system are shown, along with the trajectory of the extended ground-state band of ^{24}Mg. The 15 MeV Q-value difference between the two entrance channels is immediately obvious. Upon closer inspection, it can be seen that at low energies the trajectory deduced from the $^{14}N + {}^{10}B$ fusion cross section lies much closer to that predicted by the corresponding optical-model calculation than was the case for the $^{12}C + {}^{12}C$ reaction. As the energy increases, however, the experimental $^{14}N + {}^{10}B$ trajectory rapidly diverges from the optical-model predictions. This behavior may imply that, while there is little direct-reaction strength for $^{14}N + {}^{10}B$ at the lowest energies measured, as the bombarding energy is increased the influence of the unpaired valence nucleons becomes more important and the direct reaction strength increases. On the other hand, the optical-model potential taken from Ref. 10 was energy independent, and was actually determined from ^{10}B elastic scattering from ^{12}C targets at $E_{c.m.} = 10$ MeV, so that it may not accurately reflect the behavior of the reaction cross section at the energies studied in the present experiment.

The critical angular momentum trajectories for the two entrance channels under consideration here do not behave as expected with respect to the saturation of the total fusion cross section, if the limit to fusion is due to a compound-nucleus related property. Just as was observed for the $^{14}N + {}^{14}N$ reaction,[2] the maximum fusion cross section is lower than anticipated from such models, and the energy at which the fusion cross section saturates also seems to be too low. As was also the case for $^{14}N + {}^{14}N$ and several other systems, the difference between the measured l_c values and those expected from a compound-nucleus limitation model is approximately equal to the maximum entrance-channel spin. However, based on the observations discussed here and in Ref. 2, a simple Q-value effect cannot be dismissed.

It is also significant that the $^{14}N + {}^{10}B$ system shows evidence of structure in its total fusion yield which is on the order of 2–3 % (Fig. 6). These fluctuations can also be seen in Fig. 9, which shows the critical angular momentum trajectory for the $^{14}N + {}^{10}B$ system. In this figure, small fluctuations are seen at excitation energies of (39.6), 40.7, 42.7, 44.5, 45.1, and 47.5 MeV, approximately corresponding to $l_c = (7)$, 8, 9, 9.6, 10, and 11. In the excitation function for total fusion, these fluctuations are located at center-of-mass energies of (10.8), 11.9, 13.9, 15.7, 16.3, and 18.7 MeV. It is interesting to note that most of the observed structures correspond to consecutive integral l values, unlike the situation for $^{12}C + {}^{12}C$ where symmetry permits only even l values to contribute. One of the structures listed above, at $E_x = 45.1$ MeV ($E_{c.m.} = 16.3$ MeV), is strong and narrow. This anomaly is seen in most (but not all) of the individual yield functions for the various residual nuclei, although in some of the excitation functions it appears to be slightly wider than in others. It is particularly prominent, for example, in the yield functions for ^{21}Ne and ^{18}F (Figs. 2 and 3). It is unlikely that this structure is due to a resonance in the ^{21}Ne yield from the contaminant $^{14}N + {}^{16}O$ reaction. Not only would this require a deviation of approximately a factor of 2.5 from the average yield of ^{21}Ne from $^{14}N + {}^{16}O$, but also the $^{14}N + {}^{16}O$ cross sections were measured in this region with a comparable step size, and at the same beam energies used for the $^{14}N + {}^{10}B$ measurements, and no such deviation was observed. This structure might possibly be related to a similar "resonance" seen in the $^{12}C + {}^{20}Ne$ system at $E_x = 41.7$ MeV, which was associated with an odd critical l value. (The $E_x = 45.1$ MeV structure in the present work is apparently associated with $l_c = 10$.) In both cases, the "resonance" appears in close proximity to the point at which

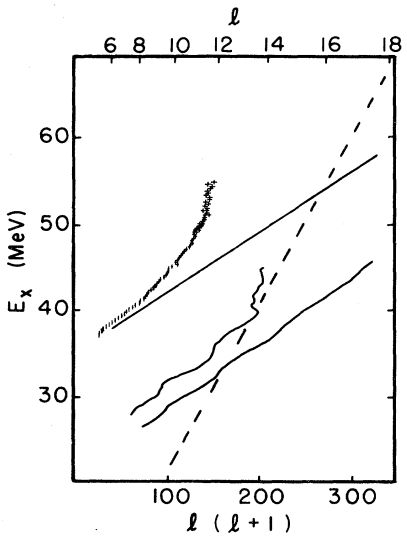

FIG. 8. The critical angular momentum trajectory for $^{14}N + {}^{10}B$ deduced from the fusion cross sections. Also shown is the trajectory for $^{12}C + {}^{12}C$ taken from Ref. 11, the trajectories deduced from the reaction cross sections calculated with the optical-model potentials of Refs. 10 and 13, and the extended ground state band of ^{24}Mg.

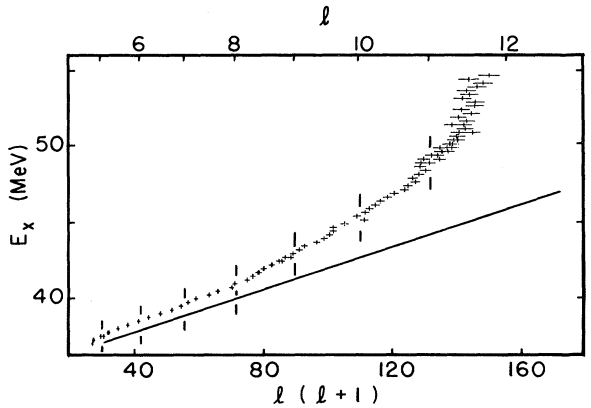

FIG. 9. The critical angular momentum trajectory for $^{14}N + {}^{10}B$ deduced from the fusion cross section, and from the theoretical reaction cross section calculated with the potential of Ref. 10. The small vertical lines indicate integral values of l_c.

the critical angular momentum trajectory changes slope. We note, however, that the "characteristic" resonance discussed in Ref. 1, usually seen in direct reaction channels near this saturation point, was not observed in the present system.

Finally, we note that a resonantlike structure has been reported by L'Ecuyer *et al.*[12] in the summed α cross sections for the $^{10}B(^{14}N,\alpha)^{20}Ne$ reaction measured at $\theta_{lab}=0°$. The observed anomaly appears to be at least a doublet, with major components located at $E_{c.m.}=9.6$ and 10.9 MeV. There is no clear evidence for either of these two structures in any of the excitation functions obtained in the present experiment. The ^{20}Ne yield does show a broad maximum at $E_{c.m.}=12$ MeV, but this may well correspond to the peak of the single-α-evaporation excitation function superimposed on a slowly rising direct transfer or four-particle-evaporation (2p2n) yield.

IV. CONCLUSION

Excitation functions for the production of nineteen residual nuclei have been measured for the $^{14}N + ^{10}B$ system over the energy range $8 \leq E_{c.m.} \leq 26$ MeV. A comparison of the individual exit channels with previous results for the $^{12}C + ^{12}C$ system at either equal compound nuclear excitation energies or equal center-of-mass energies reveals little similarity. However, it should be remembered that these two entrance channels are extremely poorly matched in terms of energy and angular momentum. As has previously been observed for other systems,[1,2,11,14] the $^{14}N + ^{10}B$ reaction exhausts most of the predicted reaction cross section in the barrier region, but saturation of the fusion yield occurs at an energy and a magnitude less than expected from compound-nuclear limitation models. The deduced critical angular momentum differs from its expected value at and above the saturation point by approximately the maximum channel spin. In light of previous work,[2,15] this behavior might well be related to the nonclosed-shell nature of the participating nuclei.

The resonant structures in the α-particle yields for the $^{10}B + ^{14}N$ reaction at $E_{c.m.}=10$ MeV reported by L'Ecuyer *et al.* did not appear either in the total fusion cross section nor in the excitation function for production of ^{20}Ne. The characteristic structure associated with the saturation of the fusion cross section in other systems[1,11,14] was also not observed. On the other hand, a strong and narrow resonantlike structure was observed at $E_{c.m.}=16.3$ MeV. This anomaly bears some resemblance to a similar "resonance" in the $^{12}C + ^{20}Ne$ fusion yield.[1] Its presence in the $^{14}N + ^{10}B$ reaction cross section at an energy corresponding to extremely high level densities in the ^{24}Mg compound system is quite remarkable, suggesting the need for further experiments.

Finally, oscillations have been observed in the fusion excitation function, as well as in excitation functions for the formation of the individual residual nuclei, in spite of the very high excitation energy and corresponding high level density in the compound system achieved in the $^{14}N + ^{10}B$ reaction. These fluctuations are even more pronounced than those observed in the $^{14}N + ^{14}N$ reaction, despite the fact that the channel spin is substantially larger here. The pattern of these anomalies is similar to that expected, for example, from "shape resonances" in the optical-model potential. However, it appears to be a considerable challenge to understand how the surface transparency apparently required for the observation of such oscillations can occur in a system such as $^{14}N + ^{10}B$, which has a very high level density and presumably therefore a very large absorptive component in its optical model potential.

ACKNOWLEDGMENTS

We wish to thank Dr. F. Haas for providing the ^{10}B targets used for these measurements. This work was supported by the National Science Foundation under Grant No. PHY-80-08234.

*Present address: State University of New York at Stony Brook, Stony Brook, NY 11794.

[1]P. A. DeYoung, J. J. Kolata, R. C. Luhn, R. E. Malmin, and S. N. Tripathi, Phys. Rev. C 25, 1420 (1982).

[2]P. A. DeYoung, J. J. Kolata, L. J. Satkowiak, and M. A. Xapsos, Phys. Rev. C 26, 1482 (1982).

[3]Program SWHET obtained from Dr. R. O. Sayer, Oak Ridge National Laboratory (unpublished).

[4]J. J. Kolata, R. M. Freeman, F. Haas, B. Heusch, and A. Gallmann, Phys. Rev. C 19, 408 (1979).

[5]R. J. deMeijer, H. S. Plendl, and R. Holub, At. Data Nucl. Data Tables 13, 1 (1974); R. J. deMeijer, A. G. Drentje, and H. S. Plendl, *ibid.* 15, 391 (1975).

[6]J. J. Kolata, R. M. Freeman, F. Haas, B. Heusch, and A. Gallmann, Phys. Rev. C 21, 579 (1980).

[7]R. L. Parks, S. T. Thornton, L. C. Dennis, and K. R. Cordell, Nucl. Phys. A348, 350 (1980).

[8]Shiu-Chin Wu, J. C. Querly, and C. A. Barnes, Nucl. Phys. A312, 177 (1978).

[9]L. J. Satkowiak, P. A. DeYoung, J. J. Kolata, and M. A. Xapsos, Phys. Rev. C 26, 2027 (1982).

[10]U. C. Voos, W. vonOertzen, and R. Bock, Nucl. Phys. A135, 207 (1969).

[11]J. J. Kolata, Phys. Lett. 95B, 215 (1980).

[12]J. L'Ecuyer, R. Voldees, C. Cardinal, L. Deschênes, and N. Marquardt, Phys. Rev. C 12, 1878 (1975).

[13]W. Reilly, R. Wieland, A. Gobbi, M. W. Sachs, and D. A. Bromley, Nuovo Cimento 13A, 913 (1973).

[14]J. J. Kolata, R. M. Freeman, F. Haas, B. Heusch, and A. Gallmann, Phys. Rev. C 19, 2237 (1979); J. J. Kolata, R. C. Fuller, R. M. Freeman, F. Haas, B. Heusch, and A. Gallmann, *ibid.* 16, 891 (1977).

[15]J. F. Mateja, A. D. Frawley, L. C. Dennis, K. Abdo, and K. W. Kemper, Phys. Rev. C 25, 2963 (1982); J. F. Mateja, R. L. Kozub, J. Garman, A. D. Frawley, L. C. Dennis, and K. W. Kemper, Bull. Am. Phys. Soc. 27, 478 (1982).